

# Stacked Catalytic Membrane Microreactor for Nitrobenzene Hydrogenation

Ming Liu, Xun Zhu, Qiang Liao,\* Rong Chen, Dingding Ye, and Gang Chen



Cite This: *Ind. Eng. Chem. Res.* 2020, 59, 9469–9477

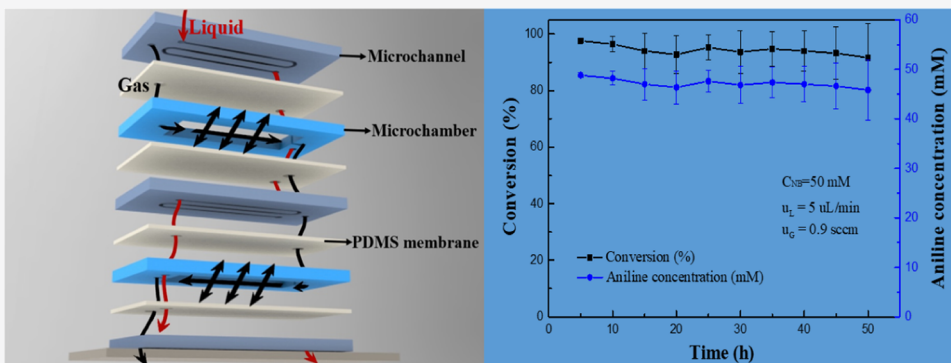


Read Online

ACCESS |

Metrics & More

Article Recommendations



**ABSTRACT:** In the present study, a novel stacked catalytic membrane microreactor assembled by microfluidic sheets and gas-permeable membranes was developed for gas–liquid–solid multiphase catalytic reactions. The developed microreactor consisted of multilayered perforated microchannels for supplying liquid reactants and perforated microchambers for supplying gas reactants, which were separated by poly(dimethylsiloxane) membranes with coated catalysts. Gas and liquid reactants flowed through their independent passageways layer by layer. Gas reactants bidirectionally permeated through the gas-permeable membrane to the catalyst layer, improving the gas utilization. Catalyst layers were prepared and immobilized on the membranes through layer-by-layer self-assembly and in situ reduction technology. Unlike other stacked microreactors, the integration of microchannels, microchambers, and membranes into one unit circumvented flow maldistribution, low durability, and low throughput of the microreactor. Furthermore, the scale-up of the membrane microreactor could be easily realized by increasing the number of microfluidic sheets and membranes. The catalytic performance was evaluated by nitrobenzene hydrogenation over palladium nanocatalyst. Results showed that the stacked catalytic membrane microreactor enabled a stable and efficient operation for 50 h. As the number of stacked layers was increased, the durability was continuously increased. The conversion was increased with increasing hydrogen flow rate or decreasing nitrobenzene flow rate. In addition, the increased inlet nitrobenzene concentration led to more serious catalyst deactivation, which decreased the conversion. In general, the stacked catalytic membrane microreactor developed in this study creates a new approach to design membrane microreactors for multiphase catalytic reactions.

## 1. INTRODUCTION

Microreactors are promising in biological engineering, medical applications, material syntheses, and the chemical industry.<sup>1–4</sup> Especially for chemical reactions, miniaturized dimensions can enhance heat and mass transfers, ensure good contact of reactants and rapid reactions,<sup>5–7</sup> and reduce explosive risks. All of these merits render chemical reactions in microreactors safe, green, and highly efficient.<sup>8–13</sup> However, for gas–liquid–solid multiphase reactions, the mass transfer limitation at the gas–liquid interface still exists in conventional microreactors.<sup>14,15</sup> To overcome this drawback, a membrane microreactor that combines the advantages of the membrane technology and microreactor has been proposed,<sup>16–19</sup> which can intensify mass transfer and realize suprarequilibrium conversions by the continuous removal of the products. More importantly,

miniaturization of the membrane reactor facilitates the attainment of optimum conditions for scale-up production.<sup>20</sup> To date, membrane microreactors have attracted wide interest and undergone rapid development. For example, Park and Kim<sup>21</sup> investigated the oxidative Heck reaction through a dual-channel membrane microreactor, in which oxygen could diffuse from one microchannel to another one to increase

Received: March 11, 2020

Revised: April 27, 2020

Accepted: April 28, 2020

Published: April 28, 2020



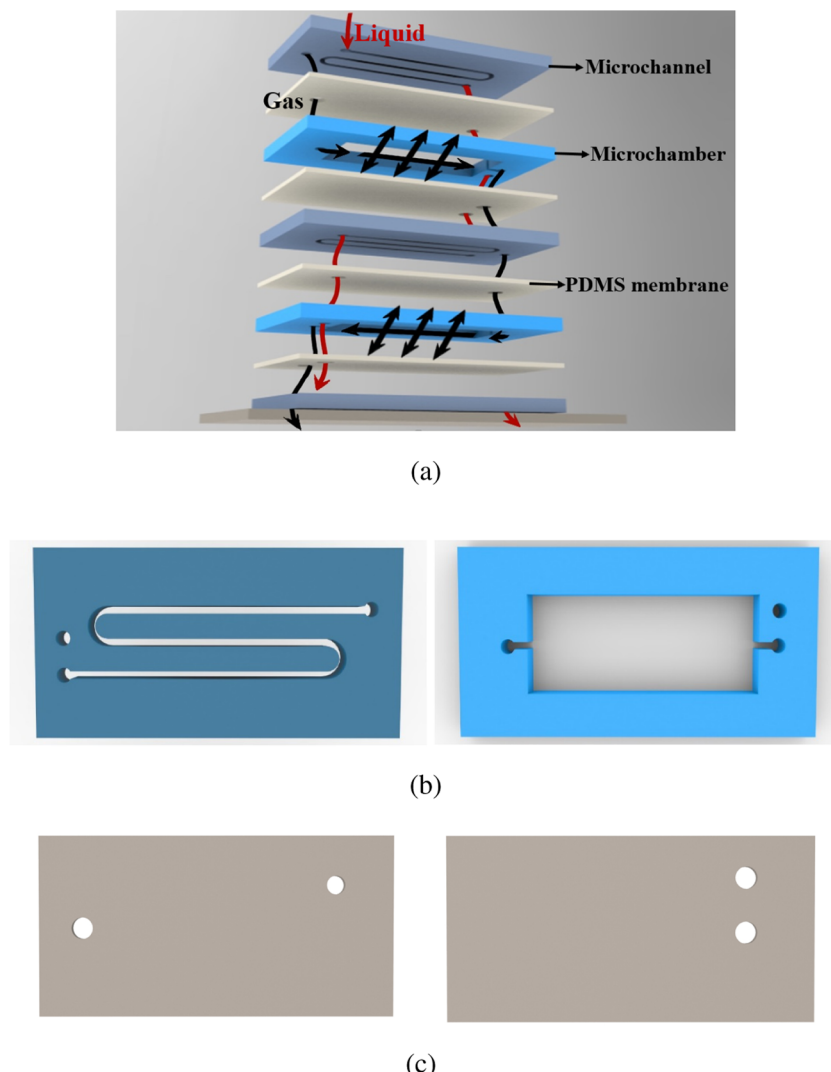


**Figure 1.** Schematic illustrations of (a) stacked catalytic membrane microreactor, (b) independent perforated microchannel and microchamber, and (c) two patterns of the PDMS membrane with two holes.

the yield and selectivity due to the increased gas–liquid contact. Liu et al.<sup>22</sup> presented a hollow-fiber catalytic membrane microreactor with a tube-in-tube design, which improved the performance of nitrobenzene hydrogenation. Chen et al.<sup>23</sup> developed a mesoporous CdS/TiO<sub>2</sub>/SBA-15@carbon paper composite membrane microreactor to enhance the visible-light-responsive photocatalytic reduction of CO<sub>2</sub>. These efforts have demonstrated membrane microreactors as powerful tools for multiphase catalytic reactions; however, the low throughput, gas utilization, and durability of these microfluidic systems still hinder the applications of this technique.

To the best of our knowledge, some stacked microreactors have been proposed to improve the throughput. Terazaki et al.<sup>24</sup> developed a glass multilayered microreactor for methanol reforming, which was used to provide hydrogen for a proton exchange membrane fuel cell. Hiramatsu et al.<sup>25</sup> investigated a microreactor equipped with stacked etched membranes for methanol steam reforming and improving the catalytic activity. Kuhn et al.<sup>26</sup> prepared a stacked microreactor that consisted of a piezoelectric actuator and microchannel to handle solid formation reactions. An ultrasonic wave was applied by a piezoelectric actuator to reduce particle deposition and

microchannel clogging. Kikutani et al.<sup>27</sup> constructed a pile-up glass microreactor stack by integrating independent microreactors. The output could be adjusted by controlling the number of stacked reactors. These works have demonstrated that the stacked membrane microreactors are able to significantly improve the throughput.

However, although these studies have attempted to investigate the stacked structure of microreactors, the flow maldistribution of the reactants in these stacked microfluidic devices still exists, which causes nonuniform heat and mass transfers and thereby lower yields with abundant byproducts. To address this issue, a stacked catalytic membrane microreactor was developed for a gas–liquid–solid three-phase catalytic reaction in this study. As illustrated in Figure 1a, the perforated microchannels for the liquid reactant supply (Figure 1b) and the perforated microchambers for the gas reactant supply (Figure 1b) are stacked to form a stacked system. Gas-permeable membranes are sandwiched between adjacent microchannels and microchambers, which separate the reactants with different phases. In this case, each microchamber faces two gas-permeable membranes positioned at its bottom and top, respectively. With this design, the multilayered structure allows the reactants to continuously flow

from the upstream to the downstream and the liquid and gas reactants flow into their respective routes without direct contact. Moreover, gas can permeate through the membranes at both sides to the catalyst layers and react with liquid reactants. It should be noted that the nearby gas-permeable membranes and microfluidic sheets all have connected holes (Figure 1c), which could allow for easy improvement in the system throughput by increasing the number of microfluidic sheets and gas-permeable membranes. In this stacked catalytic membrane microreactor, a single-phase fluid flow can be achieved by introducing membranes that can guarantee a uniform flow distribution. In this work, poly(dimethylsiloxane) (PDMS) was selected as the membrane material due to its superiority with respect to gas permeability and chemical stability.<sup>28–31</sup> The catalysts were prepared and immobilized on the PDMS membranes by the layer-by-layer (LbL) self-assembly method<sup>32–35</sup> and in situ reduction technology without corrosion. Prior to the preparation of the catalysts, dopamine and polyelectrolyte multilayers (PEMs)<sup>36,37</sup> were deposited on the PDMS membranes to adsorb metal ions. After reduction, metal nanoparticles were accordingly synthesized and grafted onto the PDMS membranes. Through this process, a stacked catalytic membrane microreactor was developed. The advantages of this type microreactor include a large reaction surface area, high gas utilization, high throughput, and easy scale-up. Therefore, the stacked catalytic membrane microreactor is effective for multiphase catalytic reactions. The performance of the stacked membrane microreactor was evaluated by nitrobenzene hydrogenation in the presence of the metal palladium (Pd).

## 2. EXPERIMENTAL SECTION

### 2.1. Design of the Stacked Membrane Microreactor.

To construct a stacked structure, the microreactor was fabricated by combining the perforated microchannel sheets, perforated microchamber sheets, PDMS membranes, and cover plates. The perforated microchannels and microchambers were machined by poly(methyl methacrylate) (PMMA) substrates, which were supplied by Xiaoniao Co. (Hangzhou, China). As shown in Figure 1b, each perforated microchannel sheet with a serpentine channel had one inlet and one outlet for the liquid reactant, and a tiny hole with a diameter of 2.0 mm was drilled next to the microchannel inlet for the gas reactant. The volume of the microchannel was 165.4  $\mu\text{L}$  with a length of 165.4 mm, a width of 1.0 mm, and a height of 1.0 mm. Similar to the microchannel, the perforated microchamber sheet had an inlet and an outlet for the gas reactant. A small hole was drilled next to the microchamber outlet with a diameter of 2.0 mm for the liquid reactant. The microchamber had a length of 32 mm, a width of 27 mm, and a height of 1 mm. A thin PDMS membrane was fabricated by the spin coating method.<sup>38,39</sup> Briefly, the PDMS prepolymer was poured onto a poly(tetrafluoroethylene) (PTFE) plate and rotated at a speed of 1200 rpm for 35 s using a spin coater (KW-4A, Xinyou, China). After curing it on a hot plate at 120 °C for 20 min, a PDMS membrane with a thickness of ~50  $\mu\text{m}$  was formed.

In this experiment, three microchannels and two microchambers were alternately stacked and four PDMS membranes were sandwiched between the adjacent microchannels and microchambers. As shown in Figure 1c, the PDMS membranes were drilled with two holes in two patterns for the gas and liquid flow into their respective passages. During the operation,

liquid reactants only flowed through microchannels, while gas flowed along the microchambers. As illustrated in Figure 1a, when the liquid phase flowed out of the upper microchannel, it passed through the tiny hole of the PDMS membrane and flowed into the inlet of the lower microchannel. The holes in the PDMS membrane and microchamber guaranteed the desired flow path of liquid reactant. As for the gas reactant, it first flowed into the small holes that settled in the first microchannel sheet and the neighboring PDMS membrane until it arrived at the first microchamber. The remaining flow path was similar to the liquid reactant. On the top and bottom of the stacked structure, two cover plates were fabricated via the PDMS substrate, and holes were drilled to the structure as inlets and outlets. Furthermore, to avoid leakage, all layers were bonded together with glue.

### 2.2. Preparation of the Pd Catalyst Layer.

The Pd catalyst layer was prepared by the LbL self-assembly and in situ reduction method. As previously mentioned, the catalyst layer was immobilized on the surface of the PDMS membranes at the liquid side. First, 30 mL of dopamine aqueous solution containing 60 mg of dopamine hydrochloride (Aladdin, China) and 36.3 mg of tris (hydroxymethyl) aminomethane (Gen-View) was injected into the microchannels with a flow rate of 30  $\mu\text{L}/\text{min}$  for 9 h. Next, the microchannels were washed with deionized water and dried by a nitrogen stream. Thus, a polydopamine (PDA) coating could be formed on the PDMS membranes by self-polymerization. After the formation of the PDA coating, PEMs of poly(sodium 4-styrenesulfonate) (PSS,  $M_w = 70\,000$ , Sigma-Aldrich, China) and poly(allylamine hydrochloride) (PAH,  $M_w = 17\,500$ , Sigma-Aldrich, China) were alternatively deposited on the PDA coating layer by layer. One should note that the PDA coating had abundant functional groups, especially catechol, amino, and phenolic hydroxyl groups.<sup>40,41</sup> The amino groups can be protonated when the pH is below 4.<sup>42</sup> Hence, the pH of the PSS aqueous solution containing 0.02 M PSS and 0.5 M NaCl (Chuangdong, China) was set to 3.5 by hydrochloric acid (HCl, Kelong, China) and sodium hydroxide (NaOH, Chuangdong, China) to enhance the interplay between the PDA and PSS in this study. To deposit the PSS and PAH on the PDA, the PSS solution was first fed into the microchannel at a flow rate of 50  $\mu\text{L}/\text{min}$  for 1 h and then rinsed by deionized water. After that, a diluted PAH aqueous solution containing 0.02 M PAH and 0.5 M NaCl was injected into the microchannel at a flow rate of 50  $\mu\text{L}/\text{min}$  for 1 h, followed by washing with deionized water to remove residual polyelectrolytes. The PSS and PAH were bonded together through electrostatic interactions, and this process was repeated three times to obtain sufficient charge carriers for the adsorption of metal ions. Then, 10 mM of  $\text{H}_2\text{PdCl}_4$  containing palladium chloride ( $\text{PdCl}_2$ , Sino-Platinum Metals, China) and 20 mM HCl was injected into the microchannel at a flow rate of 5  $\mu\text{L}/\text{min}$  for 10 h and rinsed by deionized water. The complex  $\text{PdCl}_4^{2-}$  ions were then successfully adsorbed on the PEM coatings. Thereafter, a fresh 10 mM sodium borohydride ( $\text{NaBH}_4$ , Aladdin, China) aqueous solution was injected into the microchannel at a flow rate of 30  $\mu\text{L}/\text{min}$  for 1 h to reduce the adsorbed complex  $\text{PdCl}_4^{2-}$  ions to Pd nanoparticles. Finally, the prepared Pd catalyst layer was rinsed with deionized water and dried by a nitrogen stream.

### 2.3. Experimental Setup.

The stacked catalytic membrane microreactor developed in this study was assessed by the nitrobenzene hydrogenation. Figure 2 shows a schematic

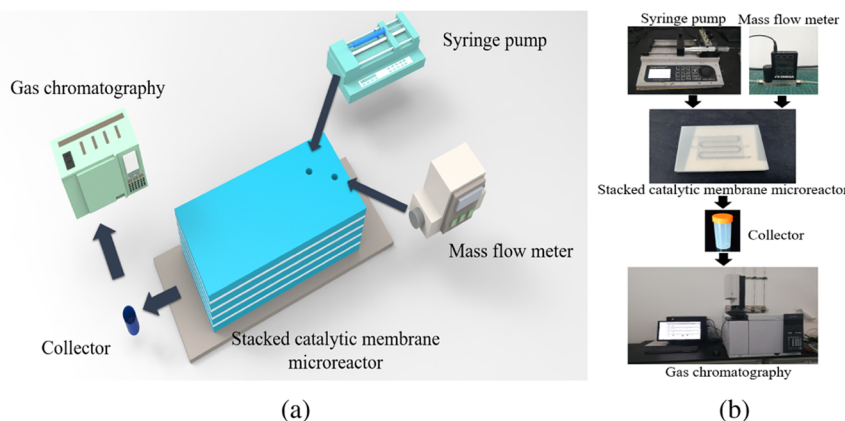


**Figure 2.** (a) Schematic illustration and (b) photographic image of the experimental system.

illustration of the experimental setup and the photographic image of the system. A mass flow controller (FMA-2602A-I, Omega) was used to supply hydrogen to the microchambers, while nitrobenzene (NB, Aladdin, China) in ethanol aqueous solution was injected into the microchannels by a syringe pump (LSP01-1BH, Longer, China). During the measurement, the NB solution and hydrogen gas were fed into the microreactor simultaneously. The effluents were collected at the outlet and measured by a gas chromatograph (7890B, Agilent) equipped with a split/splitless injection unit (SPL), a capillary column (HP-S, 30 m × 0.32 mm), and a flame ionization detector (FID). Throughout the experiment, the reaction occurred at room temperature ( $\sim 25^\circ\text{C}$ ) and atmospheric pressure. Moreover, the chemical compositions of the raw and modified PDMS membranes were analyzed by X-ray photoelectron spectroscopy (XPS, Thermo) with  $\text{Al K}\alpha$  radiation ( $h\nu = 1486.6\text{ eV}$ ) at a power of 150 W. The morphologies of the modified PDMS membrane at different steps were characterized by a scanning electron microscope (SEM, JSM-7800F, Jeol, Japan), where all of the samples were sputtered with gold.

### 3. RESULTS AND DISCUSSION

#### 3.1. Materials Characterization.

Figure 3 shows the XPS results of four spectra over a range of 200–600 eV. Two peaks

Compared to the spectrum of PDMS/PDA/PEMs, two Pd 3d peaks clearly appeared in the spectrum of the catalytic membrane (red line), which demonstrated that the  $\text{PdCl}_4^{2-}$  ions adhered to the PEMs and were successfully reduced by  $\text{NaBH}_4$ . In general, the XPS results illustrated that the PDMS membrane has been successfully modified with PDA and PEMs, and metallic Pd was successfully synthesized and immobilized on the modified PDMS membrane.

The photographic images of raw and modified PDMS membranes are given in Figure 4a,b, respectively. It was found that the raw PDMS membrane is transparent, while it changed to dark gray after modification by PDA and PEMs. In addition, the SEM images of the raw and modified PDMS membranes were also captured. As shown in Figure 4c, the raw PDMS membrane was smooth without any raised and depressed structures. After a PDA film was grafted onto the membrane, a uniform ravine structure was observed, as shown in Figure 4d. Figure 4e illustrates the surface of the PDMS membrane coated with PDA and PEMs. Compared to Figure 4d, there was no obvious difference between them. This could be attributed to the critically thin thickness of the PEMs, which was unable to change the morphology. After the  $\text{PdCl}_4^{2-}$  complex ions were reduced, the Pd nanoparticles were uniformly dispersed on the surface of the membrane, as shown in Figure 4f. From these results, it is further confirmed that each coating and Pd nanoparticles have been successfully prepared by this simple way.

#### 3.2. Performance Evaluation of the Stacked Catalytic Membrane Microreactor.

In this study, hydrogenation of NB to aniline was carried out to evaluate the catalytic performance of the stacked catalytic membrane microreactor with three microchannels, two microchambers, and four PDMS membranes. The operation was carried out under the inlet NB concentration of 50 mM, and the liquid and gas flow rates of 5  $\mu\text{L}/\text{min}$  and 0.9 sccm, respectively. Figure 5 shows the catalytic performance of the stacked catalytic membrane microreactor. The conversion remained stable with an average value higher than 90% during the 50 h operation, demonstrating good catalytic activity and durability of the developed membrane microreactor. In summary, this membrane microreactor system ensured a long-term operation with high conversion, presenting a feasible approach for heterogeneous catalytic reactions.

To gain insights into the effect of the stacked structure, two additional catalytic membrane microreactors were fabricated using the same method for comparison. One microreactor had

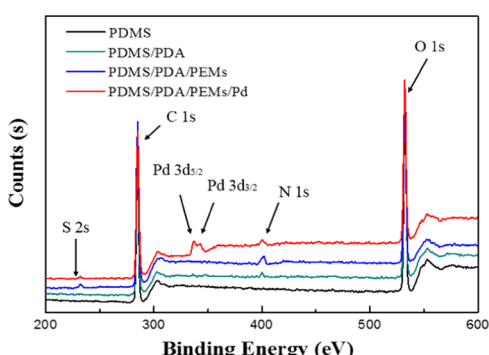


**Figure 3.** XPS spectra of raw and modified PDMS membranes.

corresponding to C 1s and O 1s appeared in the spectrum of the raw PDMS (black line). The N 1s peak that appeared after the PDA coating was grafted onto the PDMS membrane (green line). After depositing the PEMs of PSS and PAH, a peak corresponding to S 2s was observed (blue line).

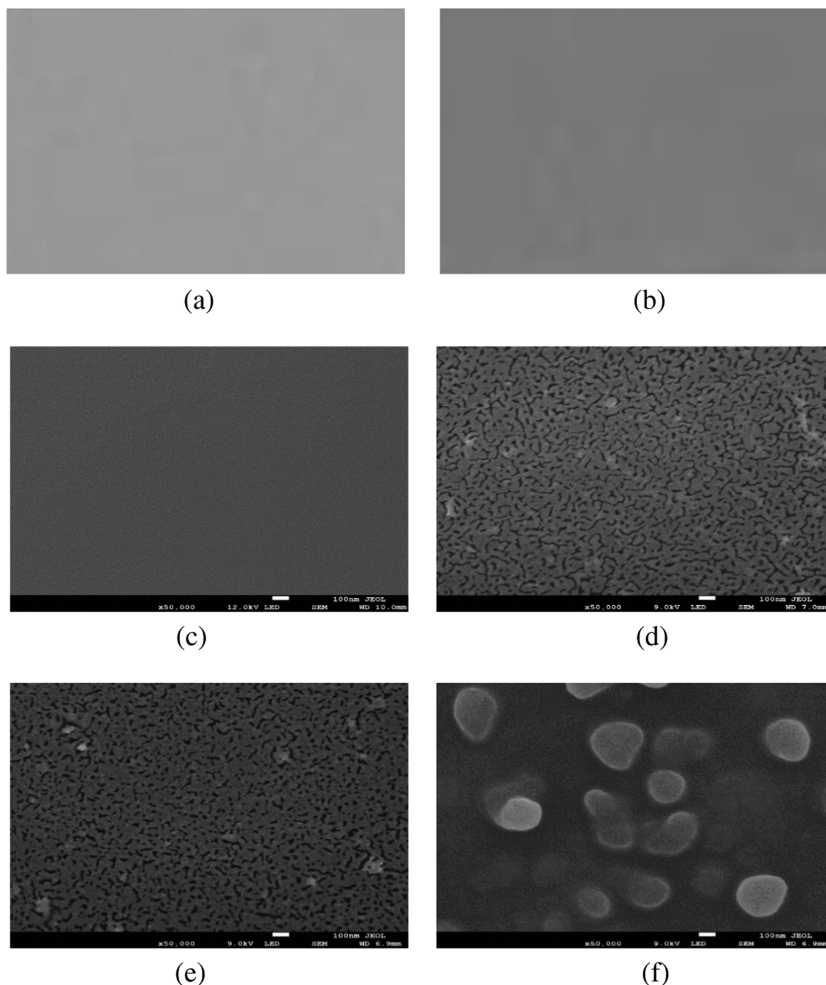


**Figure 4.** Photographic images of (a) raw PDMS membrane and (b) modified PDMS membrane. SEM images of (c) raw PDMS membrane, (d) PDMS membrane with PDA, (e) PDMS membrane with PDA and PEMs, and (f) PDMS membrane with PDA, PEMs, and Pd.

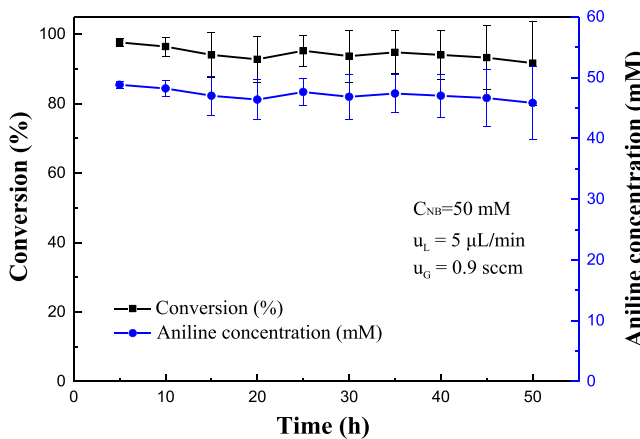


**Figure 5.** Catalytic performance of the stacked catalytic membrane microreactor.

a three-layer structure including one perforated microchannel, one perforated microchamber, and one PDMS membrane, which was referred to as the three-layer membrane microreactor (TMM). Another catalytic membrane microreactor consisted of two perforated microchannels, one perforated microchamber, and two PDMS membranes and was also constructed via stacking. These components were integrated to

form a five-layer membrane microreactor, which was referred to as the five-layer membrane microreactor (FMM). The preparation process of the catalyst layer was the same as the above-mentioned processes. Figure 6 shows the catalytic performance of the TMM and FMM. For the TMM, the initial NB conversion was 78%. Over time, the conversion gradually decreased to 24% after 10 h operation. Neither the conversion nor the durability was satisfactory. By increasing the number of microchannels from one to two, namely, FMM, the corresponding conversion and durability were upgraded.

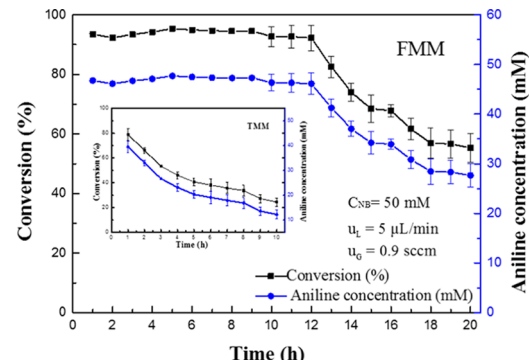


**Figure 6.** Catalytic performance of the TMM and FMM.

The NB conversion of the FMM was maintained above 90% in the first 12 h and then declined to 55% in the next 8 h. Clearly, the membrane microreactor with more multilayers presented better performance. The enhancement of the conversion and durability could be attributed to the stacked structure, which increased the reaction time, catalyst loading, and hydrogen utilization. Hence, the throughput can be easily improved by increasing the stacked unit.

To confirm the increased catalyst loading, the Pd adsorptions of the three membrane microreactors were characterized by UV-visible spectroscopy (T6-1650E, Press, China) to estimate the amount of  $\text{PdCl}_4^{2-}$  complex ions before and after the  $\text{H}_2\text{PdCl}_4$  solutions were injected into the three membrane microreactors. The peak of the  $\text{PdCl}_4^{2-}$  spectrum was observed at 425 nm,<sup>43</sup> as illustrated in Figure 7. After the

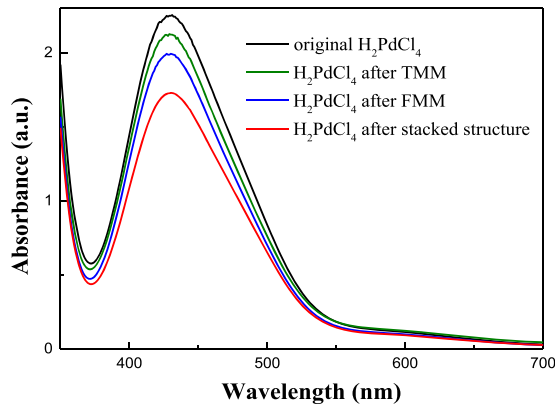


**Figure 7.** UV-vis spectra of the  $\text{H}_2\text{PdCl}_4$  solution before and after adsorption on the TMM, FMM, and stacked catalytic membrane microreactor.

original  $\text{H}_2\text{PdCl}_4$  solution flowed out from the TMM, the peak showed a slight decline, demonstrating that some  $\text{PdCl}_4^{2-}$  complex ions were adsorbed onto the PDMS membranes. Clearly, compared to the TMM, the  $\text{PdCl}_4^{2-}$  adsorptions on the FMM and stacked membrane microreactors were increased due to the increased microchannels, which indicated that the Pd loading was increased.

Another important factor that affects the performance is hydrogen utilization. Because the reaction of nitrobenzene hydrogenation is fast, the hydrogen permeated through the membrane can be rapidly and completely consumed. The amount of permeated hydrogen can be used to characterize the hydrogen utilization. In this work, an experiment was performed in the stacked catalytic membrane microreactor to estimate the amount of permeated hydrogen. Here, hydrogen was fed into the microchamber at a flow rate of 0.9 sccm, while nitrogen was simultaneously injected into the microchannel as the carrier gas at a flow rate of 1 sccm. The hydrogen permeated to the microchannel side was collected and tested by a gas chromatograph (TRACE1300, Thermo). The hydrogen permeation rate reached 0.025 mL/min, which was calculated based on the volume of the microchannel and the content of hydrogen on the microchannel at each time interval. For the microchannel sandwiched between adjacent microchambers, the permeated hydrogen was increased to 0.032 mL/min because hydrogen in the microchamber can permeate through the membranes at both sides into the microchannels. As a result, benefiting from the stacked design, hydrogen utilization could be improved. The above facts fully reveal that

the stacked catalytic membrane microreactor is favorable for the gas–liquid–solid multiphase catalytic reactions.

**3.3. Effect of Gas Flow Rate.** To study the effect of the gas flow rate, the inlet NB concentration and liquid flow rate were kept at 50 mM and 5  $\mu\text{L}/\text{min}$ , respectively. The hydrogen flow rate ranged from 0.1 to 0.9 sccm in this testing. As shown in Figure 8, the initial conversion only reached 36.8% when the

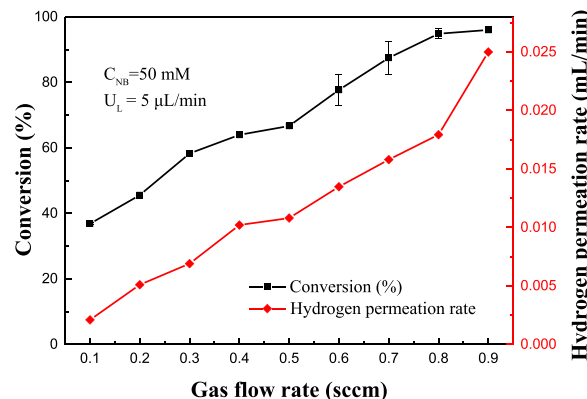


**Figure 8.** Effect of gas flow rate on the conversion and hydrogen permeation rate.

gas flow rate was 0.1 sccm. By increasing the gas flow rate to 0.9 sccm, the corresponding conversion was increased to 95.9%. Moreover, the hydrogen permeation rate to the one-side microchannel varied from 0.0021 to 0.025 mL/min as the gas flow rate increased. This increase is mainly because an increase in the hydrogen flow rate increased the pressure on the side of the microchamber, which caused more hydrogen to permeate through the PDMS membrane to the catalyst layer. If the hydrogenation is fully completed, the theoretically required minimum hydrogen can be calculated by the equation

$$U_g = \frac{nU_1 C_{\text{nb}} M_g}{\rho_{g,\text{STP}}}, \text{ where } U_1 \text{ is the NB flow rate, } n \text{ is the stoichiometric ratio of hydrogen to NB, } C_{\text{nb}} \text{ is the inlet NB concentration, } M_g \text{ is the molar weight of hydrogen, } 2 \text{ g/mol, and } \rho_{g,\text{STP}} \text{ is the hydrogen density, } 0.0899 \text{ g/L, at the standard pressure and temperature of } 101.325 \text{ kPa and } 273.15 \text{ K, respectively.}$$

After calculation,  $U_g$  was approximately 0.016 sccm. Therefore, the hydrogen permeation rate was clearly insufficient when the gas flow rate was only 0.1 sccm. As the gas flow rate increased to 0.7 sccm, the permeated hydrogen had already approached its theoretical minimum hydrogen flow rate. With a further increase in the gas flow rate, the PDMS membrane was significantly swollen due to the greatly increased pressure, leading to a faster increase in the permeation rate.<sup>44–46</sup> Correspondingly, the conversion approached the maximum. The above results and analysis indicate that the variation in the gas flow rate significantly affects the hydrogen permeation rate. Once the permeated hydrogen is sufficient, the conversion could achieve a high level.

**3.4. Effect of Liquid Flow Rate.** The aniline production rate is a key evaluation index for the performance of the stacked catalytic membrane microreactor. The effect of the liquid flow rate on the NB conversion and aniline production rate was studied. Here, the inlet NB concentration and hydrogen flow rate were maintained at 50 mM and 0.9 sccm, respectively. As shown in Figure 9, although the increase of the liquid flow rate could enhance the mass transport of liquid

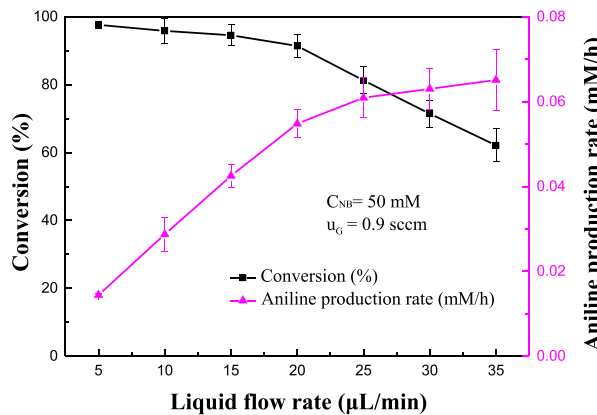


**Figure 9.** Effect of liquid flow rate on the conversion and aniline production rate.

reactant, the NB conversion decreased from nearly 100 to 62% as the liquid flow rate increased from 5 to 35  $\mu\text{L}/\text{min}$ . Notably, the NB conversion could still remain above 90% when the liquid flow rate was increased to 20  $\mu\text{L}/\text{min}$ . In fact, the change of the liquid flow rate affects not only the mass transport but also the residence time, which is the ratio of the microchannel volume to the liquid flow rate. The increase of the liquid flow rate would decrease the residence time of the NB solution. When the liquid flow rate increased to 35  $\mu\text{L}/\text{min}$ , the residence time was 14.1 min. On the other hand, because of the large surface-to-volume ratio, the mass transport was greatly enhanced and the diffusion timescale was in a few seconds.<sup>47–49</sup> The residence time was much higher than the diffusion timescale so that it is one of the predominant parameters affecting the reaction. Moreover, as the liquid flow rate increased, the hydrogen permeation rate would decrease because of the increased pressure at the liquid side. Thanks to the stacked structure of the catalytic membrane microreactor, this device not only facilitates the utilization of hydrogen but also effectively prolongs the residence time compared to conventional catalytic membrane microreactors.<sup>14,50,51</sup> Therefore, the conversion could maintain at a high level. In addition, as the liquid flow rate increased, the catalyst leaching was not found in this testing. When the liquid flow rate was 35  $\mu\text{L}/\text{min}$ , no Pd from the effluents was found according to inductively coupled plasma-optical emission spectrometry (ICP-OES) (7500ce, Agilent) measurement. It was meant that the catalyst layer was stable even operating with a high liquid flow rate. Figure 9 also shows the relationship between the liquid flow rate and the aniline production rate, which is defined as the outlet aniline concentration multiplying with the liquid flow rate. When the liquid flow rate was increased from 5 to 35  $\mu\text{L}/\text{min}$ , the aniline production rate increased from 0.014 to 0.065 mM/h. It was meant that even though the conversion decreased with the increased liquid flow rate, the throughput was still increased. Increasing the liquid flow rate could promote the mass transport of liquid reactant from the bulk to the catalyst layer so that more aniline could be produced. Meanwhile, the increase of the liquid flow rate diluted the reactant and thus the outlet aniline concentration was decreased. However, the contribution of the increased liquid flow rate was more significant. Therefore, the aniline production rate increased with increasing liquid flow rate. However, considering that both the ideal product aniline and NB dissolved in the solution, it was necessary to avoid

additional purification treatments for practical applications. Thus, a liquid flow rate of 20  $\mu\text{L}/\text{min}$  may be suitable for continuous production.

**3.5. Effect of Inlet Nitrobenzene Concentration.** The inlet NB concentration could affect the performance of the stacked catalytic membrane microreactor. To verify this point, the effect of the inlet NB concentration was investigated, ranging from 50 to 130 mM. Meanwhile, the flow rates of the gas and liquid were maintained at 5  $\mu\text{L}/\text{min}$  and 1 sccm, respectively, to ensure sufficient reaction time and hydrogen in this measurement. Figure 10 shows the variation of the

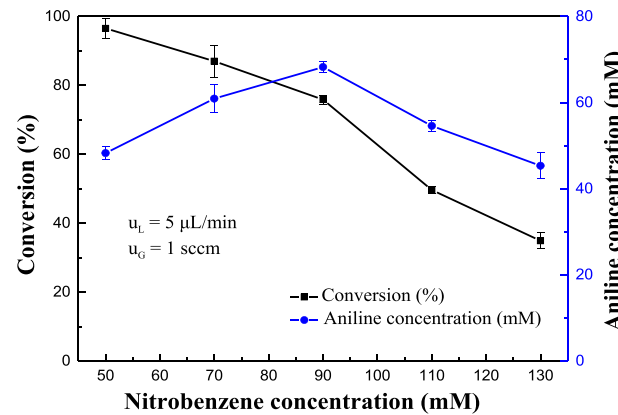


**Figure 10.** Effect of inlet nitrobenzene concentration on the conversion and aniline concentration.

conversion and aniline concentration with the inlet NB concentration. When the inlet NB concentration was 50 mM, the conversion reached 96.5% and the aniline concentration was 48.2 mM. As the inlet NB concentration increased, the conversion decreased, while the aniline concentration first increased and then decreased. Not surprisingly, the conversion gradually decreased with increasing inlet NB concentration due to the limited capacity of the microreactor. Furthermore, the highest concentration of aniline was achieved at the inlet NB concentration of 90 mM. This phenomenon was due to the combination of the enhanced mass transfer and catalyst poisoning. Increasing the inlet NB concentration could enhance the mass transport, which was helpful for the nitrobenzene hydrogenation. However, the catalyst poisoning was also aggravated as the reactant concentration increased. More intermediates and byproducts, such as nitrosobenzene and azoxybenzene, can be produced at a high concentration and thus cover the active sites.<sup>52</sup> Therefore, the yield of this microreactor was gradually decreased after it reached its limit. Given the flow rates, even though increasing the inlet NB concentration had a negative effect on the conversion in the testing range, the obtained aniline reached maximum under an intermediate inlet NB concentration.

## 4. CONCLUSIONS

In this study, a novel stacked catalytic membrane microreactor consisting of independent perforated microchannels, perforated microchambers, and PDMS membranes was proposed for nitrobenzene hydrogenation. Here, three microchannels and two microchambers were alternatively assembled together layer by layer to form a stacked structure, and four PDMS membranes were sandwiched between the adjacent micro-

channels and microchambers. Tiny holes were drilled in the microfluidic sheets and PDMS membranes for the purpose of connecting the outlets of the upstream and the inlets of the downstream. With the introduction of the gas-permeable membranes, the liquid and gas were separated and flowed into the microchannels and microchambers, respectively. The Pd nanocatalysts were synthesized on the side of microchannels by the layer-by-layer self-assembly and in situ reduction technology. With this design, gas could bidirectionally permeate through the PDMS membranes to the catalyst layer and react with the liquid to improve hydrogen utilization and throughput. This stacked configuration was structurally simple and easily expandable. The resultant catalyst layer with a uniform distribution of Pd nanoparticles was confirmed by XPS and SEM. Furthermore, the catalytic performance results were obtained by comparing them with the TMM and FMM. As the number of stacked layers was increased, the conversion and durability of the catalytic membrane microreactor increased because of the improved residence time, catalyst loading, and hydrogen utilization. Moreover, the stacked catalytic membrane microreactor maintained the conversion above 90% for 50 h. Benefiting from the stacked structure, this new type of microreactor had a certain degree of tolerance with regard to the flow rates of the gas and liquid and the inlet NB concentration. Increasing the gas flow rate led to a high hydrogen concentration in the catalytic layer as a result of increased hydrogen permeation and thus improved the NB conversion. Increasing the liquid flow rate reduced the conversion, but the aniline production rate was gradually improved. In addition, it was also found that the conversion decreased with increasing inlet NB concentration. The aniline concentration first increased because of the enhanced mass transfer and then decreased due to the deactivation of the catalyst. All of these findings have fully demonstrated that the incorporation of a stacked structure into the catalytic membrane microreactor shows a promising perspective for the multiphase catalytic reactions. Further improvement in the throughput can be easily achieved by adding more units, presenting its wide range of applications.

## AUTHOR INFORMATION

### Corresponding Author

**Qiang Liao** — Key Laboratory of Low-Grade Energy Utilization Technologies and Systems (Chongqing University), Ministry of Education, Chongqing 400030, China; Institute of Engineering Thermophysics, School of Energy and Power Engineering, Chongqing University, Chongqing 400030, China;  
✉ [orcid.org/0000-0001-9651-1160](https://orcid.org/0000-0001-9651-1160); Phone: 0086-23-65102479; Email: [lqzx@cqu.edu.cn](mailto:lqzx@cqu.edu.cn); Fax: 0086-23-65102474

### Authors

**Ming Liu** — Key Laboratory of Low-Grade Energy Utilization Technologies and Systems (Chongqing University), Ministry of Education, Chongqing 400030, China; Institute of Engineering Thermophysics, School of Energy and Power Engineering, Chongqing University, Chongqing 400030, China

**Xun Zhu** — Key Laboratory of Low-Grade Energy Utilization Technologies and Systems (Chongqing University), Ministry of Education, Chongqing 400030, China; Institute of Engineering Thermophysics, School of Energy and Power Engineering, Chongqing University, Chongqing 400030, China;  
✉ [orcid.org/0000-0003-3923-5977](https://orcid.org/0000-0003-3923-5977)

**Rong Chen** — Key Laboratory of Low-Grade Energy Utilization Technologies and Systems (Chongqing University), Ministry of Education, Chongqing 400030, China; Institute of Engineering Thermophysics, School of Energy and Power Engineering, Chongqing University, Chongqing 400030, China;  
✉ [orcid.org/0000-0002-8680-184X](https://orcid.org/0000-0002-8680-184X)

**Dingding Ye** — Key Laboratory of Low-Grade Energy Utilization Technologies and Systems (Chongqing University), Ministry of Education, Chongqing 400030, China; Institute of Engineering Thermophysics, School of Energy and Power Engineering, Chongqing University, Chongqing 400030, China

**Gang Chen** — Key Laboratory of Low-Grade Energy Utilization Technologies and Systems (Chongqing University), Ministry of Education, Chongqing 400030, China; Institute of Engineering Thermophysics, School of Energy and Power Engineering, Chongqing University, Chongqing 400030, China

Complete contact information is available at:  
<https://pubs.acs.org/10.1021/acs.iecr.0c01234>

### Notes

The authors declare no competing financial interest.

## ACKNOWLEDGMENTS

The authors gratefully acknowledge the financial supports of National Natural Science Foundation of China (Nos. 51620105011 and 51776026) and the Fundamental Research Funds for the Central Universities (No. 2018CDXYDL0001).

## REFERENCES

- (1) Jensen, K. F. Microreaction Engineering—Is Small Better? *Chem. Eng. Sci.* **2001**, *56*, 293–303.
- (2) Wu, M.-H.; Huang, S.-B.; Lee, G.-B. Microfluidic Cell Culture Systems for Drug Research. *Lab-on-a-Chip* **2010**, *10*, 939–956.
- (3) Hartman, R. L.; Jensen, K. F. Microchemical Systems for Continuous-Flow Synthesis. *Lab-on-a-Chip* **2009**, *9*, 2495–2507.
- (4) Feng, H.; Zhu, X.; Chen, R.; Liao, Q.; Liu, J.; Li, L. High-Performance Gas-Liquid-Solid Microreactor with Polydopamine Functionalized Surface Coated by Pd Nanocatalyst for Nitrobenzene Hydrogenation. *Chem. Eng. J.* **2016**, *306*, 1017–1025.
- (5) van Male, P.; de Croon, M. H. J. M.; Tiggelaar, R. M.; van den Berg, A.; Schouten, J. C. Heat and Mass Transfer in a Square Microchannel with Asymmetric Heating. *Int. J. Heat Mass Transfer* **2004**, *47*, 87–99.
- (6) Norton, D. G.; Wetzel, E. D.; Vlachos, D. G. Thermal Management in Catalytic Microreactors. *Ind. Eng. Chem. Res.* **2006**, *45*, 76–84.
- (7) Nieves-Remacha, M. J.; Kulkarni, A. A.; Jensen, K. F. Gas-Liquid Flow and Mass Transfer in an Advanced-Flow Reactor. *Ind. Eng. Chem. Res.* **2013**, *52*, 8996–9010.
- (8) Mason, B. P.; Price, K. E.; Steinbacher, J. L.; Bogdan, A. R.; McQuade, D. T. Greener Approaches to Organic Synthesis Using Microreactor Technology. *Chem. Rev.* **2007**, *107*, 2300–2318.
- (9) Roberge, D. M.; Ducry, L.; Bieler, N.; Cretton, P.; Zimmermann, B. Microreactor Technology: A Revolution for the Fine Chemical and Pharmaceutical Industries? *Chem. Eng. Technol.* **2005**, *28*, 318–323.
- (10) Kiwi-Minsker, L.; Renken, A. Microstructured Reactors for Catalytic Reactions. *Catal. Today* **2005**, *110*, 2–14.
- (11) Kobayashi, J.; Mori, Y.; Okamoto, K.; Akiyama, R.; Ueno, M.; Kitamori, T.; Kobayashi, S. A Microfluidic Device for Conducting Gas-Liquid-Solid Hydrogenation Reactions. *Science* **2004**, *304*, 1305.
- (12) Kockmann, N.; Thenée, P.; Fleischer-Trebes, C.; Laudadio, G.; Noël, T. Safety Assessment in Development and Operation of Modular Continuous-flow Processes. *React. Chem. Eng.* **2017**, *2*, 258–280.
- (13) Mallia, C. J.; Baxendale, I. R. The Use of Gases in Flow Synthesis. *Org. Process Res. Dev.* **2016**, *20*, 327–360.

- (14) Liu, M.; Zhu, X.; Chen, R.; Liao, Q.; Feng, H.; Li, L. Catalytic Membrane Microreactor with Pd/ $\gamma$ -Al<sub>2</sub>O<sub>3</sub> Coated PDMS Film Modified by Dopamine for Hydrogenation of Nitrobenzene. *Chem. Eng. J.* **2016**, *301*, 35–41.
- (15) Noël, T.; Hessel, V. Membrane Microreactors: Gas–Liquid Reactions Made Easy. *ChemSusChem* **2013**, *6*, 405–407.
- (16) de Jong, J.; Lammertink, R. G. H.; Wessling, M. Membranes and Microfluidics: A Review. *Lab-on-a-Chip* **2006**, *6*, 1125–1139.
- (17) Tan, X.; Li, K. Membrane Microreactors for Catalytic Reactions. *J. Chem. Technol. Biotechnol.* **2013**, *88*, 1771–1779.
- (18) Chen, X.; Shen, J. Review of Membranes in Microfluidics. *J. Chem. Technol. Biotechnol.* **2017**, *92*, 271–282.
- (19) Rahman, M. A.; García-García, F. R.; Li, K. Development of a Catalytic Hollow Fibre Membrane Microreactor as a Microreformer Unit for Automotive Application. *J. Membr. Sci.* **2012**, *390–391*, 68–75.
- (20) Berton, M.; de Souza, J. M.; Abdiaj, I.; McQuade, D. T.; Snead, D. R. Scaling Continuous API Synthesis from Milligram to Kilogram: Extending the Enabling Benefits of Micro to the Plant. *J. Flow Chem.* **2020**, *10*, 73–92.
- (21) Park, C. P.; Kim, D.-P. Dual-Channel Microreactor for Gas–Liquid Syntheses. *J. Am. Chem. Soc.* **2010**, *132*, 10102–10106.
- (22) Liu, M.; Zhu, X.; Chen, R.; Liao, Q.; Ye, D.; Zhang, B.; Liu, J.; Chen, G.; Wang, K. Tube-in-Tube Hollow Fiber Catalytic Membrane Microreactor for the Hydrogenation of Nitrobenzene. *Chem. Eng. J.* **2018**, *354*, 35–41.
- (23) Chen, R.; Cheng, X.; Zhu, X.; Liao, Q.; An, L.; Ye, D.; He, X.; Wang, Z. High-Performance Optofluidic Membrane Microreactor with a Mesoporous CdS/TiO<sub>2</sub>/SBA-15@Carbon Paper Composite Membrane for the CO<sub>2</sub> Photoreduction. *Chem. Eng. J.* **2017**, *316*, 911–918.
- (24) Terazaki, T.; Nomura, M.; Takeyama, K.; Nakamura, O.; Yamamoto, T. Development of Multi-Layered Microreactor with Methanol Reformer for Small PEMFC. *J. Power Sources* **2005**, *145*, 691–696.
- (25) Hiramatsu, H.; Sakurai, M.; Maki, T.; Kameyama, H. Stacked Etched Aluminum Flow-Through Membranes for Methanol Steam Reforming. *Int. J. Hydrogen Energy* **2017**, *42*, 9922–9929.
- (26) Kuhn, S.; Noël, T.; Gu, L.; Heider, P. L.; Jensen, K. F. A Teflon Microreactor with Integrated Piezoelectric Actuator to Handle Solid Forming Reactions. *Lab-on-a-Chip* **2011**, *11*, 2488–2492.
- (27) Kikutani, Y.; Hibara, A.; Uchiyama, K.; Hisamoto, H.; Tokeshi, M.; Kitamori, T. Pile-Up Glass Microreactor. *Lab-on-a-Chip* **2002**, *2*, 193–196.
- (28) Merkel, T. C.; Bondar, V. I.; Nagai, K.; Freeman, B. D.; Pinna, I. Gas Sorption, Diffusion, and Permeation in Poly (Dimethylsiloxane). *J. Polym. Sci., Part B: Polym. Phys.* **2000**, *38*, 415–434.
- (29) Singh, A.; Freeman, B. D.; Pinna, I. Pure and Mixed Gas Acetone/Nitrogen Permeation Properties of Polydimethylsiloxane [PDMS]. *J. Polym. Sci., Part B: Polym. Phys.* **1998**, *36*, 289–301.
- (30) Wang, G.; Zeng, Z.; Chen, J.; Xu, M.; Zhu, J.; Liu, S.; Ren, T.; Xue, Q. Ultra Low Water Adhesive Metal Surface for Enhanced Corrosion Protection. *RSC Adv.* **2016**, *6*, 40641–40649.
- (31) Guan, X.; Wang, Y.; Zhang, G.; Xin, J.; Wang, L.; Xue, Q. A Novel Duplex PDMS/CrN Coating with Superior Corrosion Resistance for Marine Application. *RSC Adv.* **2016**, *6*, 87003–87012.
- (32) Richardson, J. J.; Cui, J.; Björnalm, M.; Braunger, J. A.; Ejima, H.; Caruso, F. Innovation in Layer-by-Layer Assembly. *Chem. Rev.* **2016**, *116*, 14828–14867.
- (33) Farhat, T. R.; Hammond, P. T. Designing a New Generation of Proton-Exchange Membranes Using Layer-by-Layer Deposition of Polyelectrolytes. *Adv. Funct. Mater.* **2005**, *15*, 945–954.
- (34) Deligöz, H.; Yilmaztürk, S.; Gümuşoğlu, T. Improved Direct Methanol Fuel Cell Performance of Layer-by-Layer Assembled Composite and Catalyst Containing Membranes. *Electrochim. Acta* **2013**, *111*, 791–796.
- (35) Priya, D. N.; Modak, J. M.; Raichur, A. M. LbL Fabricated Poly (Styrene Sulfonate)/TiO<sub>2</sub> Multilayer Thin Films for Environmental Applications. *ACS Appl. Mater. Interfaces* **2009**, *1*, 2684–2693.
- (36) Liu, J.; Zhu, X.; Liao, Q.; Chen, R.; Ye, D.; Feng, H.; Liu, M.; Chen, G. Layer-by-Layer Self-Assembly of Palladium Nanocatalysts with Polyelectrolytes Grafted on the Polydopamine Functionalized Gas-Liquid-Solid Microreactor. *Chem. Eng. J.* **2018**, *332*, 174–182.
- (37) Yang, H.; Zhang, Q.; Zou, H.; Song, Z.; Li, S.; Jin, J.; Ma, J. Layer-by-Layer Fabrication of Polydopamine Functionalized Carbon Nanotubes-Ceria-Palladium Nanohybrids for Boosting Ethanol Electrooxidation. *Int. J. Hydrogen Energy* **2017**, *42*, 13209–13216.
- (38) Peng, Y.-T.; Lo, K.-F.; Juang, Y.-J. Constructing a Superhydrophobic Surface on Polydimethylsiloxane via Spin Coating and Vapor–Liquid Sol–Gel Process. *Langmuir* **2010**, *26*, 5167–5171.
- (39) Santisteban, T. S.; Zengerle, R.; Meier, M. Through-Holes, Cavities and Perforations in Polydimethylsiloxane (PDMS) Chips. *RSC Adv.* **2014**, *4*, 48012–48016.
- (40) Lee, H.; Dellatore, S. M.; Miller, W. M.; Messersmith, P. B. Mussel-Inspired Surface Chemistry for Multifunctional Coatings. *Science* **2007**, *318*, 426.
- (41) Yu, B.; Liu, J.; Liu, S.; Zhou, F. Pdop Layer Exhibiting Zwitterionicity: A Simple Electrochemical Interface for Governing Ion Permeability. *Chem. Commun.* **2010**, *46*, 5900–5902.
- (42) Liu, Y.; Ai, K.; Lu, L. Polydopamine and its Derivative Materials: Synthesis and Promising Applications in Energy, Environmental, and Biomedical Fields. *Chem. Rev.* **2014**, *114*, 5057–5115.
- (43) Basavegowda, N.; Mishra, K.; Lee, Y. R. Ultrasonic-Assisted Green Synthesis of Palladium Nanoparticles and their Nanocatalytic Application in Multicomponent Reaction. *New J. Chem.* **2015**, *39*, 972–977.
- (44) Lamberti, A.; Marasso, S. L.; Cocuzza, M. PDMS Membrane with Tunable Gas Permeability for Microfluidic Applications. *RSC Adv.* **2014**, *4*, 61415–61419.
- (45) Xu, R.; Zou, L.; Lin, P.; Zhang, Q.; Zhong, J. Pervaporative Desulfurization of Model Gasoline Using PDMS/BTESE-derived Organosilica Hybrid Membranes. *Fuel Process. Technol.* **2016**, *154*, 188–196.
- (46) Suleman, M. S.; Lau, K. K.; Yeong, Y. F. Development, Characterization and Performance Evaluation of A Swelling Resistant Membrane for CO<sub>2</sub>/CH<sub>4</sub> Separation. *J. Nat. Gas Sci. Eng.* **2018**, *52*, 390–400.
- (47) Swarts, J. W.; Kolschoten, R. C.; Jansen, M. C. A. A.; Janssen, A. E. M.; Boom, R. M. Effect of Diffusion on Enzyme Activity in A Microreactor. *Chem. Eng. J.* **2010**, *162*, 301–306.
- (48) Helisaz, H.; Babaei, M.; Sadeghi, A. Theoretical Modeling of Transient Reaction-diffusion Dynamics in Electrokinetic Y-shaped Microreactors. *Chem. Eng. Sci.* **2018**, *191*, 358–368.
- (49) Bolivar, J. M.; Valikhani, D.; Nidetzky, B. Demystifying the Flow: Biocatalytic Reaction Intensification in Microstructured Enzyme Reactors. *Biotechnol. J.* **2019**, *14*, No. 1800244.
- (50) Gouveia Gil, A.; Wu, Z.; Chadwick, D.; Li, K. Microstructured Catalytic Hollow Fiber Reactor for Methane Steam Reforming. *Ind. Eng. Chem. Res.* **2015**, *54*, 5563–5571.
- (51) Yao, H.; Wang, Y.; Luo, G. A Size-controllable Precipitation Method to Prepare CeO<sub>2</sub> Nanoparticles in a Membrane Dispersion Microreactor. *Ind. Eng. Chem. Res.* **2017**, *56*, 4993–4999.
- (52) Kataoka, S.; Takeuchi, Y.; Harada, A.; Takagi, T.; Takenaka, Y.; Fukaya, N.; Yasuda, H.; Ohmori, T.; Endo, A. Microreactor Containing Platinum Nanoparticles for Nitrobenzene Hydrogenation. *Appl. Catal., A* **2012**, *427–428*, 119–124.